*J. Biochem.* **139**, 459–470 (2006)
doi:10.1093/jb/mvj065

# Muscarinic Acetylcholine Receptors Activate TRPC6 Channels in PC12D Cells *via* $Ca^{2+}$ Store–Independent Mechanisms

**Lei Zhang[1,*], Feifan Guo[1,†], Ju Young Kim[2,3,‡] and David Saffen[1,2,3,4,§]**

*[1]Department of Neurochemistry, Faculty of Medicine, University of Tokyo, Hongo 7-3-1, Bunkyo-ku, Tokyo 113-0033; and [2]Graduate Program in Molecular, Cell and Developmental Biology, and [3]Departments of Pharmacology and [4]Psychiatry, College of Medicine and Public Health, The Ohio State University, 333 West 10th Ave., Columbus, OH 43210, USA*

Received December 3, 2005; accepted December 27, 2005

**In this paper we report that stimulation of mAChRs in PC12D cells activates $Ca^{2+}$ channels that are regulated independently of intracellular $Ca^{2+}$ stores. In nominally $Ca^{2+}$-free medium, exposure of PC12D cells to carbachol stimulates a robust influx of $Ba^{2+}$, a $Ca^{2+}$ substitute. This influx is blocked by atropine, but not by inhibitors of the nicotinic acetylcholine receptor or L-, N-, or T-type voltage-regulated $Ca^{2+}$ channels. By contrast, depletion of intracellular $Ca^{2+}$ stores with thapsigargin only weakly stimulates $Ba^{2+}$ influx. Unlike store-operated $Ca^{2+}$ channels (SOCCs), which close only after intracellular $Ca^{2+}$ stores refill, channels mediating carbachol-stimulated $Ba^{2+}$ influx rapidly close following the inactivation of mAChRs with atropine. $Ba^{2+}$ influx is inhibited by extracellular $Ca^{2+}$, by the $Ca^{2+}$ channel blocker SKF-96365, and by activation of protein kinase C (PKC). Exogenous expression of antisense RNA encoding the rat canonical-transient receptor potential $Ca^{2+}$ channel subtype 6 (TRPC6) or the N-terminal domain of TRPC6 blocks carbachol-stimulated $Ba^{2+}$ influx in PC12D cells. Expression of TRPC6 antisense RNA or the TRPC6 N-terminal domain also blocks $Ba^{2+}$ influx stimulated by 1-oleoyl-2-acetyl-*sn*-glycerol (OAG), a diacylglycerol analog previously shown to activate exogenously expressed TRPC6 channels. These data show that mAChRs in PC12D cells activate endogenous $Ca^{2+}$ channels that are regulated independently of $Ca^{2+}$ stores and require the expression of TRPC6.**

**Key words: barium, calcium, muscarinic acetylcholine receptor, PC12, TRPC6.**

Abbreviations: DAG, diacylglycerol; fura-2, 1-[2-(carboxyoxazol-2-yl)-6-aminobenzofuran-5-oxly]-2-(2′-amino-5′-methoxylphenoxy)-ethane-*N,N,N,N*-tetraacetic acid; fura-2-AM, fura-2-pentaacetoxymethyl ester; GF109203X, 2-[1-(3-dimethylaminopropyl)-indol-3-yl]-3-(indol-3-yl)-maleimide; GFP, green fluorescent protein, KRH, Krebs Ringer-HEPES; $IP_3$, inositol 1,4,5-trisphosphate; mAChR, muscarinic acetylcholine receptor; OAG, 1-oleoyl-2-acetyl-*sn*-glycerol; PMA, phorbol 12-myristate, 13-acetate; VRCC, voltage-regulated calcium channel; SOCC, store-operated calcium channel.

Activation of muscarinic acetylcholine receptors (mAChRs) in PC12D cells stimulates the influx of extracellular $Ca^{2+}$ by activating as-yet-unidentified $Ca^{2+}$ channels, which are regulated by the state of intracellular $Ca^{2+}$ stores (accompanying paper: Ebihara, Guo, Zhang, Kim and Saffen, 2006). Because our experiments showed that this pathway accounts for most, if not all, of the carbachol-stimulated $Ca^{2+}$ influx, we initially thought that these data told the entire story of mAChR-regulated $Ca^{2+}$ influx in these cells. A different picture emerged, however, when we began to use $Ba^{2+}$ as a $Ca^{2+}$ substitute in our experiments. $Ba^{2+}$ has often been used as a tracer for visualizing $Ca^{2+}$ influx, since it also increases the fluorescence of fura-2 upon binding (*1*, *2*). Unlike $Ca^{2+}$, however, $Ba^{2+}$ is not a substrate for plasma membrane $Ca^{2+}$ pumps or exchange proteins (*1*, *3*), and it therefore becomes trapped after entering the cells. $Ba^{2+}$-dependent increases in intracellular fura-2 fluorescence thus reflect the rate of $Ba^{2+}$ influx, whereas $Ca^{2+}$-dependent changes in intracellular fura-2 fluorescence reflect the balance of $Ca^{2+}$ influx and efflux. We decided to examine $Ba^{2+}$-dependent changes in intracellular fura-2 fluorescence to explore the properties of the influx component of carbachol-stimulated $Ca^{2+}$ influx in the PC12D cells.

In the experiments described below we show that the use of $Ba^{2+}$ as a $Ca^{2+}$ tracer reveals the presence of a second mAChR-regulated $Ca^{2+}$ influx pathway in PC12D cells. In contrast to the AChR-regulated SOCCs, the second pathway is not significantly activated following depletion of intracellular $Ca^{2+}$ stores with thapsigargin, but is robustly activated following activation of mAChRs with carbachol. The channels underlying the $Ca^{2+}$ store–independent pathway can be distinguished from the SOCCs by their kinetics

[§]To whom correspondence should be addressed at: Department of Pharmacology, College of Medicine and Public Health, 5072C Graves Hall, 333 West 10th Ave, Columbus, Ohio. Tel: +1-614-688-4573, Fax: +1-614-292-7232, E-mail: saffen.1@osu.edu

[*]Present address: Department of Pharmacology, University of Minnesota, 6-120 Jackson Hall, 321 Church St. S.E., Minneapolis, MN 55455, USA.

[†]Present address: Department of Biology, Pennsylvania State University, 113 Life Science Bldg, University Park, PA 16801, USA.

[‡]Present address: Department of Neuroscience/Institute for Cell Engineering, The Johns Hopkins University, BRB 729, 733 N. Broadway, Baltimore, MD 21205, USA.

 

of opening and closing, ion permeabilities and regulation by phorbol ester.

Recently, mammalian homologs of the Drosophila transient receptor potential (TRP) and TRP-like (TRPL) $Ca^{2+}$ channels (*4*) have emerged as promising candidates for the $Ca^{2+}$ channels underlying $Ca^{2+}$ store–operated and store-independent channels (*5–7*). The mammalian TRP channel superfamily comprises six families (*7*). The TRPC (canonical) family (*8*), which has the highest homology to Drosophila TRP channels, contains seven subtypes (TRPC1–7) that have been shown to form $Ca^{2+}$-permeable channels. The mechanisms by which individual TRP channel subtypes are regulated is currently the subject of intense investigation, with some studies showing activation coupled to the depletion of intracellular $Ca^{2+}$ stores [TRPC1 (*9*, *10*), TRPC3 (*11–13*) TRPC4 (*14*), TRPC5 (*15*), TRPC7 (*16*)] and others $Ca^{2+}$ store–independent regulatory mechanisms [TRPC3 (*9*, *11–13*, *17*), TRPC4 (*18*), TRPC5 (*15*, *19*), TRPC6 (*20*, *21*), TRPC7 (*22*)]. An early study by Boulay and coworkers (*20*) and our own previous study (*21*) showed that TRPC6 is activated in a $Ca^{2+}$ store–independent manner following stimulation of mAChRs. These results prompted us to test the effects of rat TRPC6 antisense and dominant-negative expression constructs on mAChR-activated $Ba^{2+}$ influx in PC12. As we describe below, inhibition of TRPC6 expression completely blocked carbachol-stimulated $Ba^{2+}$ influx in these cells. A study by Hofmann and colleagues (*23*) showed that exogenously expressed TRPC6 channels can be activated by diacylglycerol analogs, including 1-oleoyl-2-acetyl-*sn*-glycerol (OAG). Here we show that OAG also stimulates $Ba^{2+}$ influx in PC12D cells and that this influx can be blocked in cells expressing TRPC6 antisense RNA or dominant-negative constructs. Taken together, these results suggest that expression of TRPC6 channels is required for mAChR- and OAG-mediated, $Ca^{2+}$ store–independent $Ca^{2+}$ influx in PC12D cells.

## MATERIALS AND METHODS

*Materials*—Carbachol, atropine, tubocurarine, nifedipine, verapamil, ω-conotoxin GVIA, ω-agatoxin IVA, nicotine, $BaCl_2$, *N*-methyl-glutamine, thapsigargin, $MnCl_2$, $CaCl_2$, $LaCl_2$, phorbol 12-myristate 13-acetate (PMA), GF109203X, 1-oleoyl-2-acetyl-*sn*-glycerol (OAG), SKF-96365, were obtained from CalBiochem. Fura-2 and fura-2-pentaacetoxymethyl ester (fura-2-AM) were purchased from Dojin Chemical Research Labs (Kumamoto, Japan) and Sigma-Aldrich (St. Louis, MO). Krebs-Ringer-HEPES (KRH) contains: 125 mM NaCl, 5 mM KCl, 1.2 mM $KH_2PO_4$, 1.2 mM $MgCl_2$, 2 mM, $CaCl_2$, 6 mM glucose, and 25 mM HEPES- NaOH (pH 7.4). Nominally $Ca^{2+}$-free KRH was prepared by omitting $CaCl_2$; nominally $Ca^{2+}$- and $PO_4$-free KRH by omitting $CaCl_2$ and $K_2HPO_4$ and adding 0.1% gelatin.

*Cell Culture and Transfection*—PC12D cells (a generous gift from M. Sano, Kyoto Prefectural University Medical School) were grown in DMEM supplemented with 5% fetal calf serum and 5% horse serum as previously described (*24*). Non-differentiated cells were used in all of the experiments. For transfection experiments, 80–90% confluent cultures of cells were seeded in 12-well culture plates (Costar) at 40% confluency. After incubation for 24 h at 37°C (5% $CO_2$), a transfection mix containing 1 μg of control vector (pEF-BOS-SK) or 1 μg of TRPC6 antisense RNA expression vector (pEF-BOS-SK-TRPC6A-antisense) or 1 μg of N-terminal domain expression vector [pEGFP-N2-TRPC6B-N (1–310)], 50 ng of green-fluorescent protein expression vector (pEGF-N2; Clontech), 1.25 μl of Lipofectamine 2000 (Gibco-BRL), and 100 μl of Opti-MEM (Gibco-BRL) was added to each well. The cells were incubated for 24 h at 37°C (5% $CO_2$), after which the transfection mixtures were replaced with normal medium. The cells were incubated for an additional two days prior to loading with fura-2-AM for fluorescence experiments. The construction and properties of the TRPC6 antisense and N-terminal domain expression vectors are described in Ref. *21*.

*Measurement of Intracellular Fura-2 Fluorescence*—Method 1 (Figs. 1–10): Intracellular fura-2 fluorescence of PC12D cells was measured in stirred suspensions in KRH in quartz cuvettes using a Nippon Bunko/Jasco FP770 spectrofluorometer as previously described (*24*). Immediately prior to measuring $Ba^{2+}$ influx, an aliquot of fura-2 loaded cells was washed three-times with nominally $Ca^{2+}$-free KRH buffer and gently resuspended

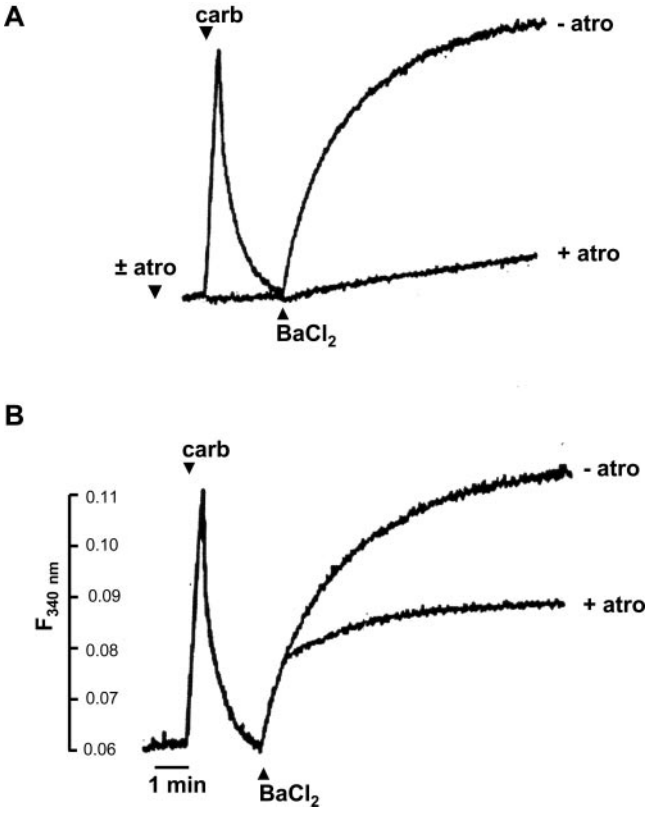


Fig. 1. **Activation of mAChRs stimulates the influx of extracellular $Ba^{2+}$; atropine blocks this influx immediately.** A and B: Changes in intracellular fura-2 fluorescence [$\lambda_{ex}$ = 340 nm; $\lambda_{em}$ = 510 nm for this and all subsequent experiments, unless indicated] were measured in stirred suspensions of PC12D cells in nominally $Ca^{2+}$-free KRH using a Nippon Bunko/Jasco FP-770 spectrofluorometer. Cells were pretreated with 50 μM tubocurarine to block nicotinic receptors prior to addition of 500 μM carbachol, 200 μM $BaCl_2$, and 10 μM atropine at the times indicated by the arrowheads. The fluorescence ($F_{340\ nm}$; arbitrary units) and time (1 min) scales apply to A and B. The traces shown are representative of more than 10 independent experiments.

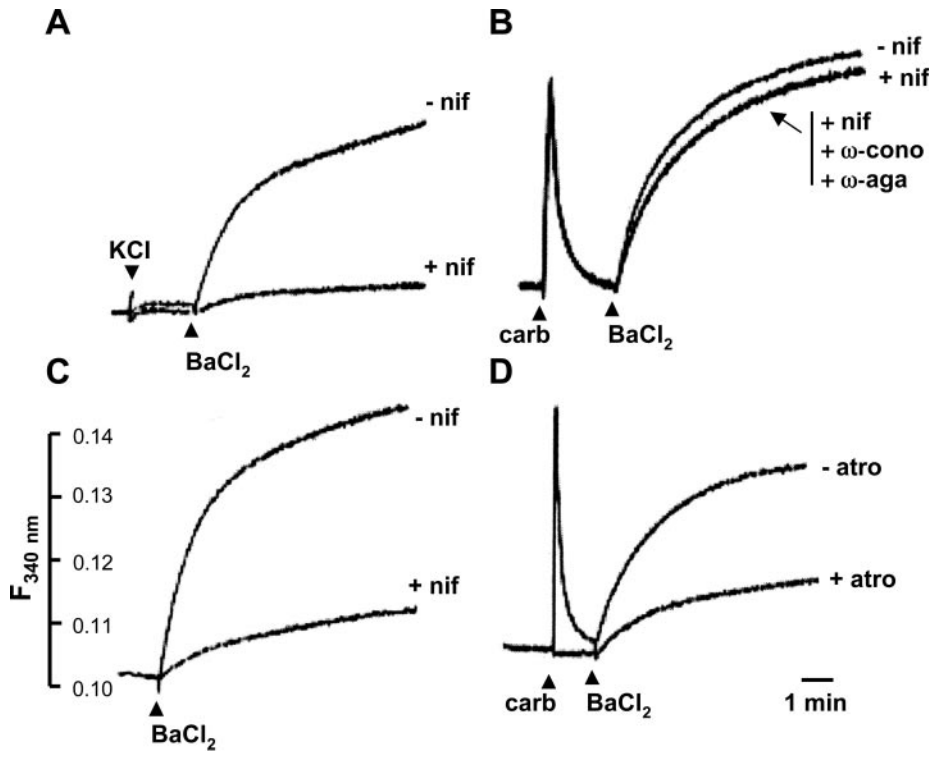


Fig. 2. **Carbachol-stimulated $Ba^{2+}$ influx is not mediated by voltage-regulated $Ca^{2+}$ channels.** A–D: $Ca^{2+}$ and $Ba^{2+}$-dependent changes in intracellular fura-2 fluorescence in PC12D cells in nominally $Ca^{2+}$-free KRH were measured as described in the legend to Fig. 1. All cells (A–D) were pretreated with 50 μM tubocurarine. A: Top and bottom traces: membrane depolarization was induced by the addition of 60 mM KCl prior to addition of 200 $BaCl_2$ μM at the times indicated. Cells were pretreated for 5 min with 1 μM nifedipine (+nif) or 0.1% DMSO (–nif). B: Cells were pretreated with 0.1% DMSO (–nif), 1 μM nifedipine (+nif), or 1 μM nifedipine, 3 μM ω-conotoxin and 50 nM ω-agatoxin (+ nif + ω-con +ω-aga) prior to the addition of 500 μM carbachol and 200 μM $BaCl_2$ at the times indicated. C: Cells in standard KRH were pretreated for 5 min with 0.1% DMSO (–nif) or 1 μM nifedipine (+nif), then resuspended in isosmotic KRH containing 120 mM KCl (in place of NaCl) and 0.1% DMSO (top trace) or 1 μM nifedipine (bottom trace). 200 μM $BaCl_2$ was added at the time indicated by the arrowhead. D: Cells were pretreated for 5 min with 1 μM nifedipine and then resuspended in isosmotic KRH containing 120 mM KCl and 1 μM nifedipine. Cells were pretreated with water (–atro) or 10 μM atropine (+atro) prior to the addition of 500 μM carbachol and 200 μM $BaCl_2$ at the times indicated. The fluorescence ($F_{340\ nm}$; arbitrary units) and time (1 min) scales apply to traces in A through D: The traces shown are representative of 6 independent experiments.

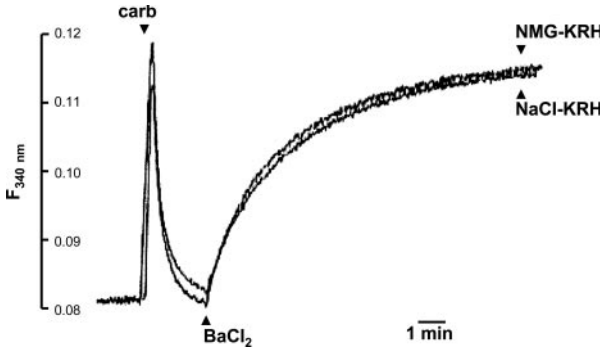


Fig. 3. **Carbachol-stimulated $Ba^{2+}$ influx does not depend upon extracellular $Na^{+}$.** Fura-2 loaded PC12D cells were resuspended in standard $Ca^{2+}$-free KRH (NaCl-KRH) or $Ca^{2+}$-free KRH containing 125 mM *N*-methyl-D-glucamine in place of NaCl (NMG-KRH). Cells were pretreated with 50 μM tubocurarine and 2 μM nifedipine prior to addition of 500 μM carbachol and 200 μM $BaCl_2$ at the times indicated by the arrows. The results shown are representative of 3 independent experiments.

at approximately $2 \times 10^6$ cells/ml in the same buffer. All measurements were carried out at 22°C. Differences in baseline values of $F_{340}$ reflect differences in the: (i) number of cells in the cuvette, (ii) efficiency of fura-2 loading, and/or (iii) spectrofluorometer settings. Maximal $Ca^{2+}$- and $Ba^{2+}$-dependent fluorescence signals were typically 50–60% of the maximal fura-2 fluorescence signal measured by lysing the cells with 0.1% Triton X-100. Composite fluorescence traces were constructed as described in the accompanying paper (Ebihara, Guo, Zhang, Kim and Saffen, 2006). Artifacts associated with the opening and closing of the cover of the cuvette chamber were omitted from the traces. Method 2 (Figs. 11 and 12): Transfected cells were grown in 12-well plates until 50–75% confluence. The attached cells were then gently washed three-times with KRH, incubated in KRH containing 2 μM fura-2-AM for 90 min to 3 h at room temperature, and gently washed three-times with nominally $Ca^{2+}$-free KRH to remove extracellular fura-2-AM and $Ca^{2+}$. Fura-2 fluorescence in single cells or small clusters of cells was then measured at room temperature as previously described (*21*) using an Argus-50/CA system

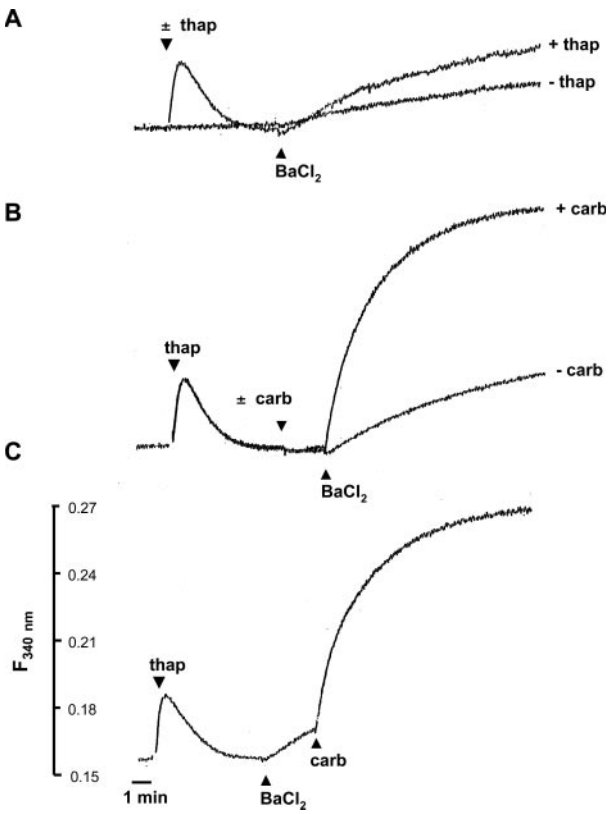


Fig. 4. **Carbachol activates the influx of extracellular $Ba^{2+}$ independently of the state of the intracellular $Ca^{2+}$ stores.** A–C: Fura-2 loaded PC12D cells in nominally $Ca^{2+}$-free KRH were pretreated with 50 μM tubocurarine and 1 μM nifedipine. A: Intracellular $Ca^{2+}$ stores were depleted with 100 nM thapsigargin (+thap) or treated with vehicle (DMSO; – thap) prior to addition of 200 μM $BaCl_2$. B: Cells were pretreated with water (+carb) or 10 μM atropine (–carb) prior to addition of 100 nM thapsigargin and 500 μM carbachol and 200 μM $BaCl_2$ at the times indicated by the arrowheads. C: Cells were treated with 100 nM thapsigargin, and 500 μM carbachol and 200 μM $BaCl_2$ at the times indicated. The fluorescence ($F_{340\ nm}$; arbitrary units) and time (1 min) scales apply to A through C. These results are representative of 6 independent experiments.

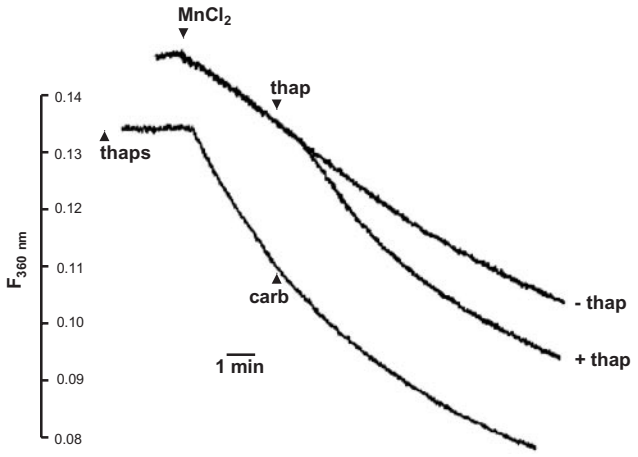


Fig. 5. **Carbachol does not increase the influx of $Mn^{2+}$ into PC12D cells pretreated with thapsigargin.** Top two traces: PC12D cells in nominally $Ca^{2+}$-free KRH were pretreated with 50 μM tubocurarine and 1 μM nifedipine prior to addition of 5 μM $MnCl_2$. A: Cells were exposed to 0.1% DMSO (– thap) or 100 nM thapsigargin (+ thap) at the times indicted by the arrowheads. Bottom trace: cells were pretreated with 100 nM thapsigargin prior to addition of 500 μM carbachol at the indicated times. The fluorescence ($F_{360\ nm}$; arbitrary units) and time (1 min) scales apply to all the traces in the figure. The position of the top two traces is offset in the upward direction for clarity. (The starting position of all the traces was the same in the actual data.) These results are representative of 3 independent experiments.

(Hamamatsu Photonics) in combination with an Olympus IMT-2 upright microscope. Calculations of fluorescence data were performed using Excel (Microsoft, Inc.) and graphs were prepared using Kaleidagraph™ (Abelbeck Software). Maximal $Ca^{2+}$- and $Ba^{2+}$-dependent fluorescence signals were approximately 60% of the maximal fura-2 fluorescence signal measured by adding 1 μM ionomycin.

## RESULTS

*Activation of mAChRs Stimulates the Influx of Extracellular $Ba^{2+}$* via *Channels That Are Distinct from the Nicotine Acetylcholine Receptor, Voltage-Gated $Ca^{2+}$ Channels, and the $Na^+/Ca^{2+}$ Exchanger*—Figure 1A shows that addition of carbachol to PC12D cells in nominally $Ca^{2+}$-free KRH induces the rapid release of $Ca^{2+}$ from internal stores and stimulates a robust influx of extracellular $Ba^{2+}$. This $Ba^{2+}$ influx is dependent upon the activation of mAChRs, since it is blocked by atropine, but not by 50 μM tubocurarine. Figure 1B shows that blocking mAChRs with atropine shortly after the addition of $Ba^{2+}$ results in an immediate decrease in the rate of $Ba^{2+}$ influx. This rapid inhibition of $Ba^{2+}$ influx contrasts sharply with the effect of atropine on $Mn^{2+}$ influx through SOCCs, where inhibition is observed only after a lag of 60 to 90 s (Ebihara, Guo, Zhang, Kim and Saffen, 2006).

Because voltage-regulated $Ca^{2+}$ channels (VRCCs) are permeable to $Ba^{2+}$, we examined whether carbachol-stimulated $Ba^{2+}$ influx is affected by VRCC blockers. Undifferentiated PC12 cells express primarily L-type $Ca^{2+}$ channels (*25*, *26*), and only a small number of N-type (*26*) and P/Q-type (*27*) $Ca^{2+}$ channels. Figure 2A shows that $Ba^{2+}$ influx induced by membrane depolarization with 60 mM KCl is largely blocked by pretreating PC12D cells with nifedipine, an inhibitor of L-type $Ca^{2+}$ channels. Figure 2B shows that pretreating PC12D cells with nifedipine, or nifedipine plus ω-conotoxin and ω-agatoxin (which block N-type and P/Q-type $Ca^{2+}$ channels, respectively) has little effect on carbachol-stimulated $Ba^{2+}$ influx. To make sure that carbachol stimulates $Ba^{2+}$ influx through non-VRCCs, we examined the ability of carbachol to stimulate $Ba^{2+}$ influx in PC12D cells under even more highly depolarizing conditions. Figure 2C shows that $Ba^{2+}$ influx stimulated by resuspending PC12D cells in KRH containing 120 mM KCl in place of NaCl can be largely blocked by pretreating the cells with 1 μM nifedipine. Figure 2D shows that addition of carbachol to PC12D cells pretreated with nifedipine and resuspended in KRH containing 120 mM KCl still stimulates $Ba^{2+}$ influx. Results similar to those depicted in Fig. 2 were obtained with 2 and 10 μM nifedipine and 10 and 20 μM verapamil (D. Saffen, unpublished observations). Together, these results show that mAChR-stimulated $Ba^{2+}$ influx occurs via channels that are distinct from L-, N- or P/Q-type VGCC.

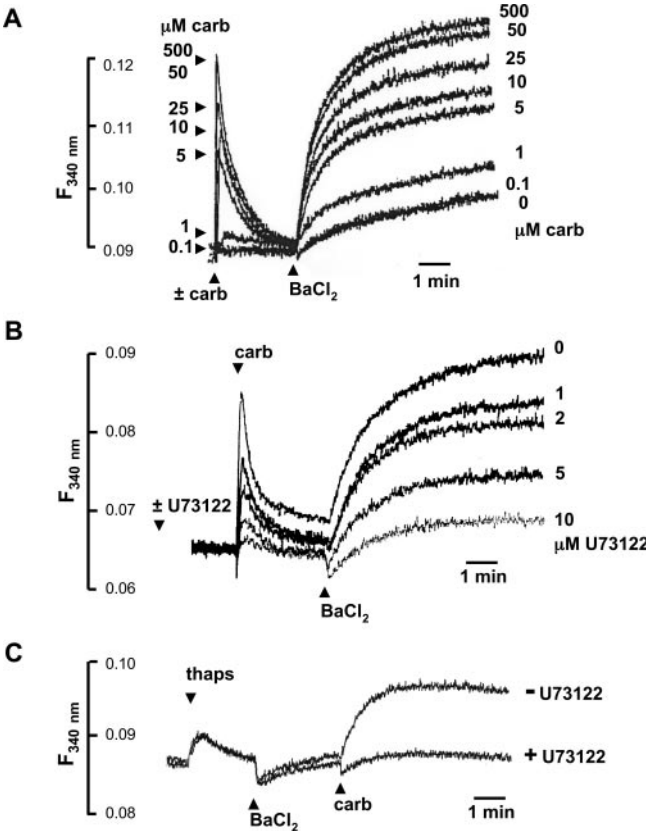


Fig. 6. **Carbachol stimulates the release of $Ca^{2+}$ from internal stores and $Ba^{2+}$ influx with similar potencies; release of $Ca^{2+}$ from internal stores and $Ba^{2+}$ influx are blocked by inhibition of PLC.** A–C: PC12D cells in nominally $Ca^{2+}$-free KRH were pretreated with 50 μM tubocurarine and 1 μM nifedipine. A: PC12D cells were exposed to the indicated concentrations of carbachol (0–500 μM) prior to addition of carbachol and 200 μM $BaCl_2$ at the times indicated by the arrows. B: PC12D cells were pretreated with 0.1% dimethylsulfoxide (–U73122) or the indicated concentrations of U73122 (0–10 μM) 4 min prior to addition of 500 μM carabachol and 200 μM BaCl2. C: PC12D cells were pretreated with 0.1% dimethylsulfoxide (–U73122) or 10 μM U73122 4 min prior to addition of 100 nM thapsigargin, 200 μM $BaCl_2$ and 500 μM carabachol and at the indicated times. Each of the results shown is representative of 2 independent experiments.

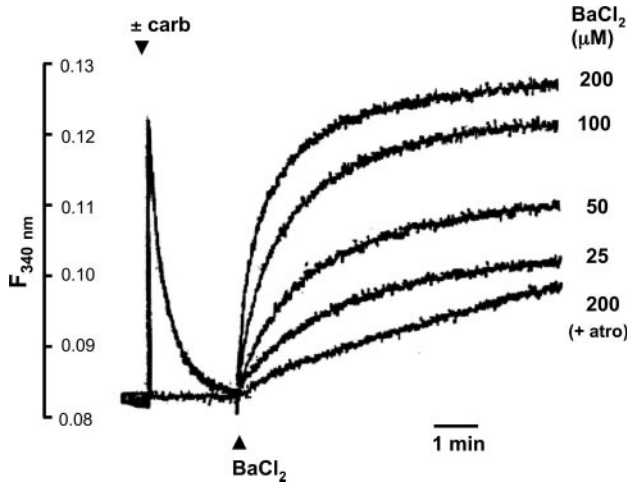


Fig. 7. **Carbachol-stimulated $Ba^{2+}$ influx is rapidly blocked.** Top four traces: PC12D cells in nominally $Ca^{2+}$-free KRH were pretreated with 50 μM tubocurarine and 1 μM nifedipine and stimulated with 500 μM carbachol prior to the addition of the indicated concentrations of $BaCl_2$. For clarity, only one $Ca^{2+}$ release trace is shown and all additional traces were aligned at the times of $BaCl_2$ addition. Bottom trace (+atro): 10 μM atropine was added prior to stimulation with 500 μM carbachol and addition of 200 μM $BaCl_2$. The traces shown are representative of 2 independent experiments.

Another potential pathway for $Ba^{2+}$ entry into cell is through the $Na^+/Ca^{2+}$ exchanger, which normally functions to expel $Ca^{2+}$ from the cell by exchanging extracellular $Na^+$ for intracellular $Ca^{2+}$, but which can also function in reverse (*28*, *29*). $Ba^{2+}$ can enter the cell *via* this exchanger and once inside cannot be expelled, resulting in $Ba^{2+}$ accumulation (*30*, *31*). Since $Ba^{2+}$ influx through the $Na^+/Ca^{2+}$ exchanger is increased at low concentrations of extracellular $Na^+$ (*30*, *31*), we examined the possible involvement of this pathway in mAChR-stimulated $Ba^{2+}$ influx by comparing carbachol-stimulated $Ba^{2+}$ influx in standard KRH and KRH containing 125 mM *N*-methyl-glutamine in place of NaCl. As shown in Fig. 3, carbachol-stimulated $Ba^{2+}$ influx was unaffected by the removal of $Na^+$, suggesting that the $Na^+/Ca^{2+}$ exchanger does not contribute significantly to this influx.

*Carbachol-Stimulated $Ba^{2+}$ Influx Is Mediated by Channels That Are Regulated Independently of the Intracellular $Ca^{2+}$ Stores*—The fact that carbachol-stimulated $Ba^{2+}$ influx is immediately blocked by atropine raised the possibility that $Ba^{2+}$ enters the cell via channels that are distinct from the SOCCs described in the accompanying paper. To determine if $Ba^{2+}$ is influenced by the state of the intracellular stores, we examined the effects of thapsigargin on $Ba^{2+}$ influx. Figure 4A shows that depletion of intracellular stores with thapsigargin causes only a small increase in $Ba^{2+}$ influx. Figure 4B and C show that pretreatment of PC12D cells with thapsigargin does not occlude the stimulation of $Ba^{2+}$ influx by carbachol and that the rate and extent of carbachol-stimulated $Ba^{2+}$ influx are much greater than that for $Ba^{2+}$ influx stimulated by thapsigargin.

In the accompanying paper (Ebihara, Guo, Zhang, Kim and Saffen, 2006), we show that carbachol and thapsigargin stimulate the influx of $Mn^{2+}$ to the same extent, and that treating cells with carbachol and thapsigargin together did not further increase the rate of $Mn^{2+}$ entry. Because those experiments were carried out with PC12D cells in standard KRH, containing 2 mM $CaCl_2$, we examined whether carbachol also increases the rate of $Mn^{2+}$ influx in nominally $Ca^{2+}$-free KRH, *i.e.*, under the same conditions used to measure $Ba^{2+}$ influx. Figure 5 (top traces) shows that exposure to thapsigargin causes an increase of $Mn^{2+}$ influx. The onset of this increase occurs approximately 60 s after the addition of thapsigargin, a delay that correlates with thapsigargin-induced emptying of intracellular $Ca^{2+}$ stores. (See Fig. 4 for time course for thapsigargin-induced depletion of intracellular $Ca^{2+}$ stores.) The observed lag in thapsigargin-stimulated $Mn^{2+}$ entry suggests that the $Mn^{2+}$-permeable channels are activated only after $Ca^{2+}$ stores become significantly depleted. Figure 5 (bottom trace) shows that pretreating cells with thapsigargin also causes an increased rate of $Mn^{2+}$ entry, but that this rate is not further increased

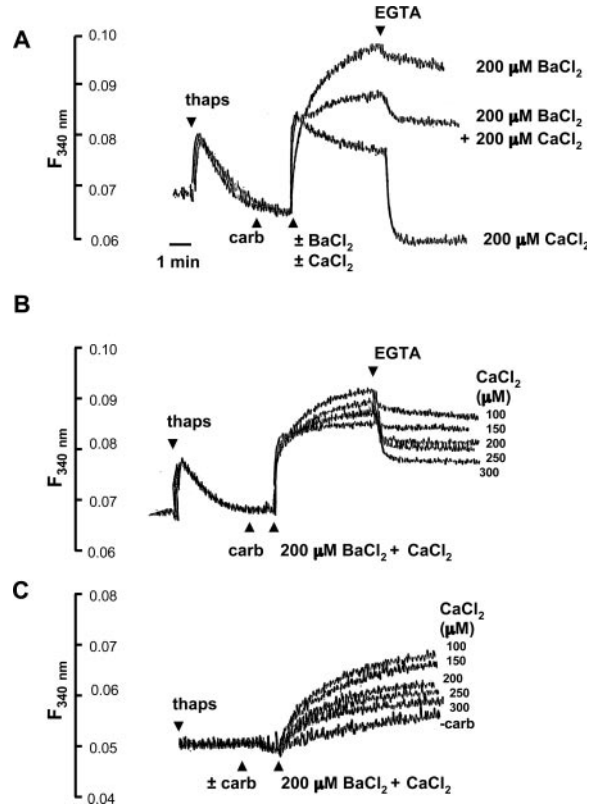


Fig. 8. **$Ca^{2+}$ dose-dependently blocks $Ba^{2+}$ influx stimulated by carbachol $Ca^{2+}$.** A and B: Fura-2 fluorescence was measured at an excitation wavelength ($\lambda_{ex}$) of 340 nm. A: PC12D cells in nominally $Ca^{2+}$-free KRH were pretreated with 50 μM tubocurarine and 1 μM nifedipine prior to addition of 400 nM thapsigargin, 500 μM carbachol and 200 μM $BaCl_2$ (top trace), 200 μM $CaCl_2$ (bottom trace). Extracellular $Ba^{2+}$ and $Ca^{2+}$ were chelated by adding 3 mM EGTA at the times indicated by the arrowheads. B: PC12D cells were pretreated with tubocurarine, nifedipine, thapsigargin and carbachol as in (A) prior the addition of 200 μM $BaCl_2$ plus the indicated concentrations of $CaCl_2$. C: Top five traces: PC12D cells were treated as in (B), except that $\lambda_{ex}$ = 360 nm. Bottom trace: cells were pretreated with atropine prior to addition of 500 μM carbachol and addition of 200 μM $BaCl_2$. The time (1 min) scale applies to A through C. The traces shown are representative of 2 independent experiments.

by the addition of carbachol. Thus, under the same conditions carbachol stimulates the robust influx of $Ba^{2+}$, but not $Mn^{2+}$. (Compare the trace in Fig. 4C and the lower trace in Fig. 5.) Together these results suggest that carbachol-stimulated $Ba^{2+}$ influx is mediated by channels distinct from the $Mn^{2+}$-permeable SOCCs that are activated by thapsigargin.

*$Ba^{+}$ Influx Is Linked to the Activation of M1 mAChRs*—We previously showed that PC12D cells express mRNAs for both M1 and M4 subtypes of muscarinic receptors, but that M1 subtype alone mediates the induction of immediate-early *zif268* (*egr-1*) gene by carbachol (*24*). M1 mAChRs couple to pertussis toxin-insensitive $G_{q/11}$ to activate PLC-β, and M4 mAChRs couple to pertussis toxin-sensitive Gi to inhibit adenylate cyclase (*32*). To gain insight into which of these mAChR subtypes are important for carbachol-stimulated $Ba^{2+}$ influx, we examined the effect of increasing carbachol concentrations on $Ba^{2+}$ influx. Figure 6A shows that both the rate and extent of $Ba^{2+}$ influx increase with increasing concentrations of carbachol. Inspection of the family of curves in Fig. 6A shows that carbachol stimulates the influx of $Ba^{2+}$ and the release of $Ca^{2+}$ from internal stores with roughly the same potency. Figure 6B shows that both carbachol-stimulated release of $Ca^{2+}$ from intracellular stores and $Ba^{2+}$ influx are blocked by increasing concentrations of U73122, a PLC-β inhibitor (*33*, *34*). Figure 6C shows that U73122 also blocks carbachol-stimulated $Ba^{2+}$ influx in cells pretreated with thapsigargin to deplete intracellular $Ca^{2+}$ stores. Taken together, these data indicate that carbachol-stimulated $Ba^{2+}$ requires the activation of M1 mAChRs and PLC-β.

*$Ba^{2+}$ Influx Is Only Transiently Stimulated by Carbachol*—Because $Ba^{2+}$ cannot be expelled from the cells, it would be expected to accumulate to the same extent regardless of its rate of entry, as long as the channels remain open. The fact that accumulation of $Ba^{2+}$ inside the cell increased with increasing concentrations of carbachol suggests, therefore, that entry is blocked shortly after stimulation of mAChRs. Data presented in Fig. 2 in our accompanying paper suggests that mAChRs remain active for at least 10 min in the continued presence of carbachol (Ebihara, Guo, Zhang, Kim and Saffen, 2006).

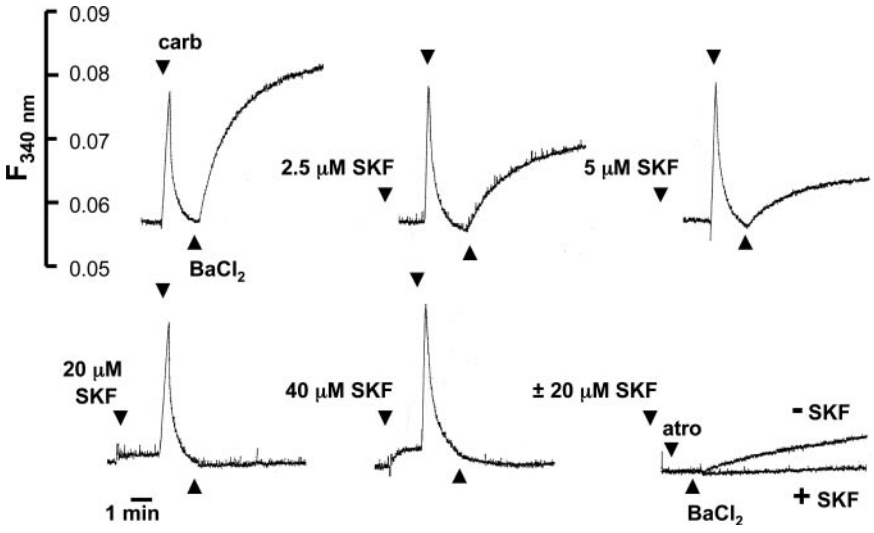


Fig. 9. **Carbachol-stimulated $Ba^{2+}$ influx is blocked by the $Ca^{2+}$ channel inhibitor SKF-39365.** PC12D cells in nominally $Ca^{2+}$-free KRH were pretreated with the indicated concentrations of SKF-96365 prior to addition of 500 μM carbachol and 200 μM $BaCl_2$ at the times indicated by the arrows. Cells in the lower right panel were pretreated with SKF-96365 and 2 μM atropine prior to adding 200 μM $BaCl_2$. The fluorescence ($F_{340\,nm}$; arbitrary units) and time (1 min) scales apply to all the traces. The results shown are representative of 3 independent experiments.

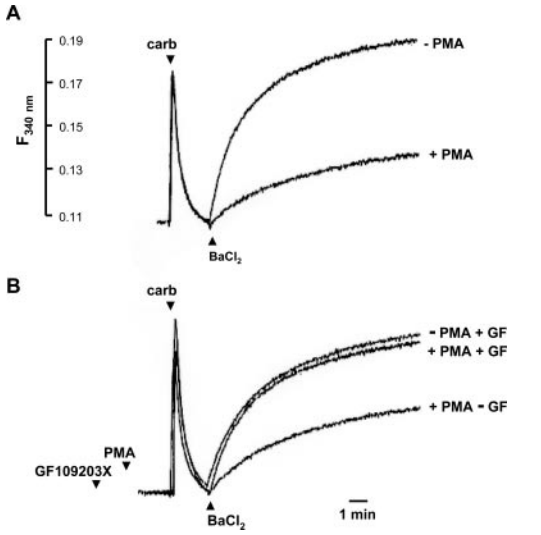


Fig. 10. **Activation of PKC inhibits carbachol-stimulated $Ba^{2+}$ influx.** A: PC12D cells in nominally $Ca^{2+}$-free KRH were pretreated with 0.1% ethanol (–PMA) or 100 nM PMA prior to addition of 500 μM carbachol and 200 μM $BaCl_2$ at the times indicated by the arrows. B: Cells were pretreated with 2 μM GF109203X (traces 1 and 2) or 0.1% DMSO (trace 3) for five min prior to addition of 100 nM PMA (traces 2 and 3), 500 μM carbachol and 200 μM $BaCl_2$ at the times indicated by the arrows. The fluorescence ($F_{340\ nm}$; arbitrary units) and time (1 min) scales apply to A and B. The results shown are representative of 5 independent experiments.

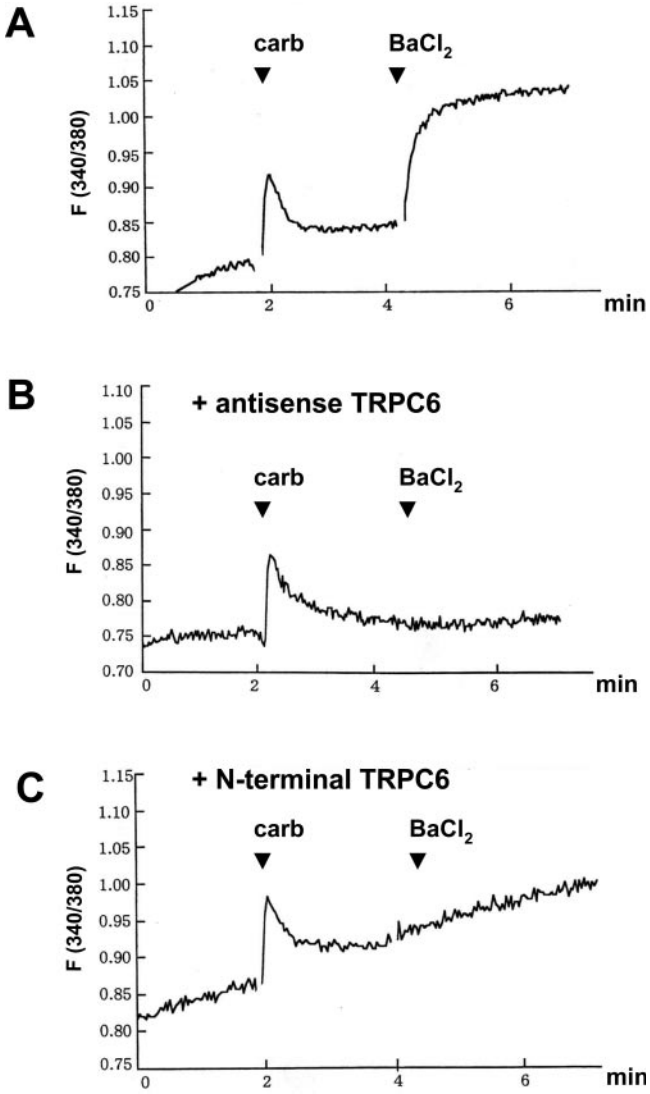


Fig. 11. **Carbachol-stimulated $Ba^{2+}$ influx is blocked in PC12D cells expressing TRP6 antisense RNA or the TRP6 N-terminal cytoplasmic domain.** Changes in intracellular fluorescence in fura-2 loaded PC12D cells were measured using the Argus-50 $Ca^{2+}$ imaging system (Hamamatsu) as described in "MATERIALS AND METHODS." Cells were transfected with the GFP expression vector pEGFP-N2 and the empty expression vector pEF-BOS-SK (A), or the TRPC6A antisense RNA expression vector pEF-BOS-SK-TRPC6A-antisense (B), or the TRP6B N-terminal domain expression vector pEGFP-N2-TRP6B-N (C) two days prior to carrying out the experiments shown. Cells in nominally $Ca^{2+}$-free KRH were exposed to 500 μM carbachol and 200 μM $BaCl_2$ at the times indicated by the arrowheads. The traces shown are averages obtained by imaging EGFP-expressing 6 single cells or cell clusters (2–4 cells) and are representative of 3 independent experiments.

Thus, the fact that $Ba^{2+}$ does not accumulate to the same extent at each concentration of carbachol suggests that the $Ba^{2+}$-permeable channels become inhibited shortly after the addition of carbachol. Consistent with this idea, Fig. 7 shows that not only the rate of $Ba^{2+}$ influx, but also maximal levels of $Ba^{2+}$ accumulation increase with increasing concentrations of extracellular $Ba^{2+}$. The observation that $Ba^{2+}$ accumulations reach a plateau within 1–2 min after the addition of $Ba^{2+}$ to the medium suggests that the $Ba^{2+}$ channels become blocked within this period of time.

*Carbachol-Stimulated $Ba^{2+}$ Influx Is Blocked by Extracellular $Ca^{2+}$*—While investigating the properties of the carbachol-stimulated $Ba^{2+}$ influx, we noticed that the influx of $Ba^{2+}$ is inhibited by extracellular $Ca^{2+}$. Figure 8 shows the effect of increasing concentrations of extracellular $Ca^{2+}$ on carbachol-stimulated $Ba^{2+}$ influx. In these experiments we pretreated the cells with thapsigargin to irreversibly deplete intracellular stores, stimulated the cells with carbachol, and then added $BaCl_2$ and $CaCl_2$ at different concentrations. $Ba^{2+}$ accumulation was assessed by chelating extracellular $Ba^{2+}$ and $Ca^{2+}$ with EGTA. Since $Ba^{2+}$ that enters the cell remains trapped inside the cell, addition of EGTA does not cause a large decrease in intracellular fura-2 fluorescence (Fig. 8A, top trace). Small decreases in fluorescence are the result of removal of $Ba^{2+}$ from extracellular fura-2 that leaked from the cells.

By contrast, $Ca^{2+}$-dependent intracellular fura-2 fluorescence depends upon the relative rates of $Ca^{2+}$ influx and efflux. Chelation of extracellular $Ca^{2+}$ causes a rapid decrease in intracellular fura-2 fluorescence, since $Ca^{2+}$ expelled from the cells cannot be replaced (Fig. 8A, bottom trace). When $Ba^{2+}$ and $Ca^{2+}$ are taken up together, addition of EGTA causes intracellular fura-2 fluorescence to drop to levels that lie between the levels obtained with $Ba^{2+}$ alone or $Ca^{2+}$ alone (Fig. 8A, middle trace). Thus, the EGTA-resistance component of the fluorescence signal is proportional to the amount of $Ba^{2+}$ that enters the cell.

Figure 8B shows that increasing concentrations of $Ca^{2+}$ reduce the EGTA-resistant component of intracellular

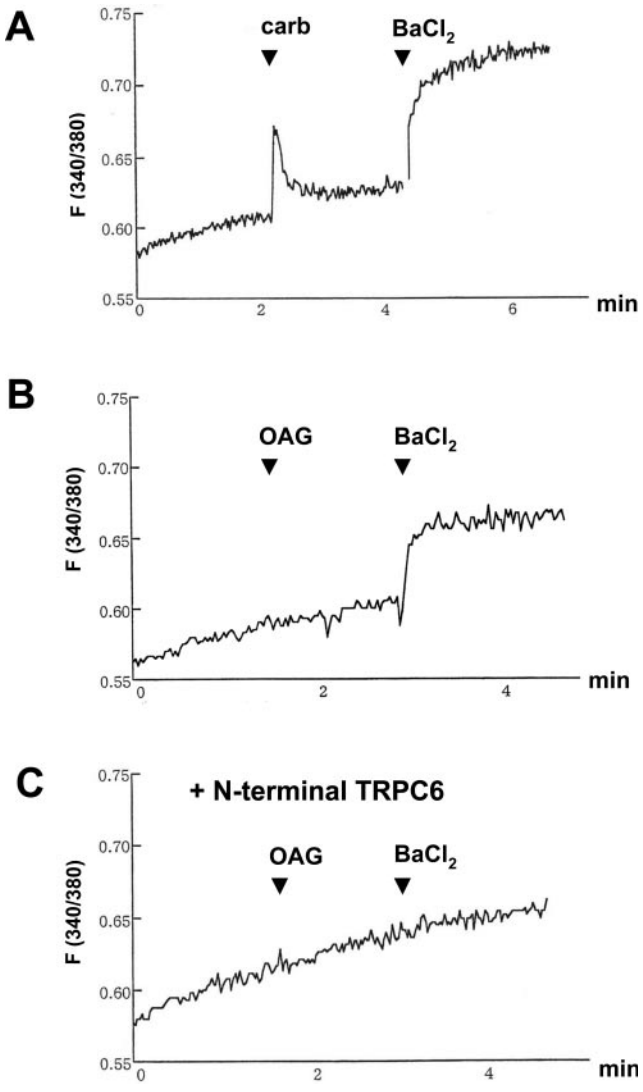


Fig. 12. **Expression of TRP6 N-terminal cytoplasmic domain blocks activation of $Ba^{2+}$ by DAG analogue OAG.** Changes in intracellular fura-2 fluorescence were measured as described in the legend to Fig. 11. Cells transfected with pEGFP-N2 and pEF-BOS-SK (A and B) or pEGFP-N2-TRP6B-N (C) in nominally $Ca^{2+}$-free KRH were exposed to 500 μM carbachol, 100 μM OAG and 200 μM $BaCl_2$ at the times indicated by the arrowheads. The results shown are representative of 3 independent experiments.

fura-2 fluorescence. The $Ba^{2+}$-component of influx can be selectively visualized by using 360 nm light to excite fura-2. Fura-2 fluorescence does not change with changes in free $Ca^{2+}$ concentrations at this wavelength [the isosbestic wavelength for $Ca^{2+}$; (*35*)], but does exhibit $Ba^{2+}$-dependent changes in fluorescence. Figure 8C shows the results of an independent experiment in which PC12D cells were treated as in Fig. 8B, but excited with 360 nm light to selectively visualize $Ba^{2+}$-dependent changes in intracellular fura-2 fluorescence. This experiment also shows that extracellular $Ca^{2+}$ blocks the entry of $Ba^{2+}$ in a dose-dependent manner.

*Carbachol-Stimulated $Ba^{2+}$ Influx Is Blocked by the $Ca^{2+}$ Channel Blocker SKF-96365*—To obtain evidence that $Ba^{2+}$-dependent increases in intracellular fura-2 fluorescence are due to the influx of $Ba^{2+}$ through a $Ca^{2+}$ channel, we examined the effects of several known $Ca^{2+}$ channel inhibitors. Figure 9 shows that carbachol-stimulated $Ba^{2+}$ influx is blocked by low concentrations of SKF-96365, an inhibitor of non-voltage gated calcium channels (*36*). Carbachol-stimulated $Ba^{2+}$ influx is also inhibited by 100 μM $LaCl_3$, a known $Ca^{2+}$ channel blocker (Guo and Saffen, unpublished observations).

*Activation of PKC Inhibits Carbachol-Stimulated $Ba^{2+}$ Influx*—While screening various compounds for the ability to block carbachol-stimulated $Ba^{2+}$ influx, we noticed that the influx was potently inhibited by phorbol esters. Figure 10A shows that pretreatment of PC12D cells with 100 nM PMA dramatically blocks the stimulation of $Ba^{2+}$ influx by carbachol, without affecting the release of $Ca^{2+}$ from intracellular stores. This inhibition is completely blocked by pretreatment with the PKC inhibitor GF 109203X, indicating that inhibition of $Ba^{2+}$ influx is caused by the activation of PKC. By contrast, pretreatment of PC12D cells with 100 nM PMA had no effect on thapsigargin-stimulated $Mn^{2+}$ entry, indicating that phorbol esters do not block activation of SOCCs (Guo and Saffen, unpublished observations). Also, pretreatment of PC12D cells with 100 nM PMA for 5 min caused only a small change in carbachol-induced $Ca^{2+}$ influx (Guo and Saffen, unpublished observation). This result suggests that $Ba^{2+}$ permeable channels make only a small contribution to carbachol-stimulated $Ca^{2+}$ influx in these cells.

*Carbachol-Stimulated $Ba^{2+}$ Influx Is Blocked by Expression of Rat TRPC6A Antisense RNA or TRPC6 N-Terminal Peptide*—RT-PCR analysis showed that PC12D cells express mRNAs for TRPC1, C3, C6 and C7 [TRPC2, C4 and C5 were not detected; Kim and Saffen, unpublished observations. By contrast, Tesfai and coworkers detected mRNA encoding TRPC1 through -C6 in PC12 cells by RT-PCR (*37*)]. Because TRPC6 exogenously expressed in HEK293 (*20*) and COS7 (*21*) cells was previously reported to be activated by mAChRs independently of the intracellular $Ca^{2+}$ stores, we decided to investigate whether this $Ca^{2+}$ channel contributed to carbachol-stimulated $Ba^{2+}$ influx in PC12D cells. For this purpose, we transfected PC12D cells with expression vectors encoding: (i) the full-length anti-sense RNA for the TRPC6A isoform (in combination with an expression vector for green fluorescent protein (GFP) to allow identification of the transfected cells) or (ii) the N-terminal domain (amino acids 1–300) of the TRPC6B isoform fused to GFP. We have previously shown that transfection of COS7 cells with the TRPC6A antisense expression vector blocks exogenous expression of TRPC6 (*21*). Expression of TRPC6 antisense RNA or the N-terminal domain was also shown to block TRPC6-mediated $Ba^{2+}$ influx in these cells (*21*). Figure 11 shows that two days after transfection, carbachol-stimulated $Ba^{2+}$ influx (Fig. 11A) is completely blocked in PC12D cells expressing full-length TRPC6 antisense RNA expression vector (Fig. 11B) or the TRPC6 N-terminal domain expression vector (Fig. 11C). By contrast, cells transfected with TRPC6 antisense or N-terminal domain expression vectors showed little change in carbachol-stimulated $Ca^{2+}$ influx (Zhang and Saffen, unpublished observations), suggesting that their inhibitor effects are specific for the $Ba^{2+}$-permeable channel.

*$Ba^{2+}$ Influx Activated by DAG Analog OAG Is Blocked by Expression of the TRPC6 N-Terminal Peptide*—As

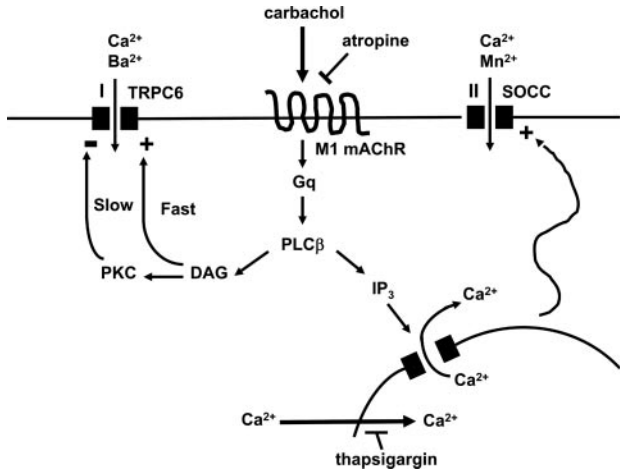


Fig. 13. **Model depicting two pathways for M1 mAChR-regulated $Ca^{2+}$ influx in PC12D cells.** In addition to the store-operated calcium channel (SOCC) pathway described in the accompanying paper (Ebihara *et al*., 2005), stimulation of M1 mAChRs in PC12D cells with carbachol activates TRPC6 calcium channels. These channels are not activated by depletion of ER $Ca^{2+}$ stores, but may be activated by DAG (on a time-scale of seconds). DAG also activates PKC, which inhibits the TRPC6 channels (on a time scale of minutes). The SOCCs are permeable to $Ca^{2+}$ and $Mn^{2+}$ and the TRPC6 channels are permeable to $Ca^{2+}$ and $Ba^{2+}$ (in the presence of low concentrations of extracellular $Ca^{2+}$).

mentioned above, TRPC6 channels can be activated by analogs of DAG (*23*). Figure 12B shows that exposure of PC12D cells to 100 μM OAG stimulates $Ba^{2+}$ influx in the absence of detectable release of $Ca^{2+}$ from internal stores. Figure 13C shows that this influx is completely blocked in PC12D cells expressing the TRPC6 N-terminal domain. Together, these results show that OAG-stimulated $Ba^{2+}$ influx requires the expression of endogenous TRPC6 channels in PC12D cells.

## DISCUSSION

In this paper we show that mAChRs in PC12D cells activate the influx of extracellular $Ba^{2+}$ *via* a pathway that is distinct from the store-operated $Ca^{2+}$ channel (SOCC)–dependent pathway described in the accompanying paper). A model incorporating the findings of both of these studies is depicted in Fig. 13.

The existence of additional mAChR-activated $Ca^{2+}$ channels in PC12D cells was surprising, since our previous experiments suggested that most if not all of the carbachol-stimulated $Ca^{2+}$ influx could be accounted for by SOCCs. In retrospect, this apparent discrepancy may be explained by the fact that the $Ba^{2+}$-permeable $Ca^{2+}$ channels make only a small contribution to mAChR-regulated $Ca^{2+}$ influx. $Ba^{2+}$ influx produces a robust increase in intracellular fura-2 fluorescence (Fig. 1A), because $Ba^{2+}$ that enters the cell becomes trapped there. By contrast, $Ca^{2+}$-dependent increases in intracellular fura-2 fluorescence reflect the balance between $Ca^{2+}$ influx and efflux. Thus, small increases in $Ba^{2+}$ influx can produce large increases in intracellular fura-2 fluorescence, while comparatively larger increases in $Ca^{2+}$ influx (relative to efflux) are required to produce increases in fura-2 fluorescence. Also, as described below, the transient time course of mAChR-stimulated $Ba^{2+}$-influx suggests that the $Ba^{2+}$-permeable channels make a contribution to mAChR-stimulated $Ca^{2+}$ influx only during the first 1–2 min following exposure to carbachol. These characteristics of the $Ba^{2+}$-permeable channels, *i.e.*, relatively small numbers and transient activation, explain why these channels make little or no contribution to the plateau phase of mAChR-stimulated Ca $^{2+}$ influx in PC12D cells.

The first indication that $Ba^{2+}$ enters the cells *via* a channel distinct from those mediating the majority of carbachol or thapsigargin-stimulated $Ca^{2+}$ influx was the observation that blocking mAChR receptors with atropine immediately slowed the entry of $Ba^{2+}$ into the cell (Fig. 1B). By contrast, store-operated $Ca^{2+}$ channels begin to close only after a lag of 60 to 90 s, the time required for the $Ca^{2+}$ stores to refill. The fact that carbachol-stimulated $Ba^{2+}$ influx was not affected by inhibitors of the nicotinic acetylcholine receptor or voltage-regulated $Ca^{2+}$ channel blockers (Fig. 2B), by a perturbation that affects the $Na^+/Ca^{2+}$ transporter (Fig. 3), or by emptying of the intracellular $Ca^{2+}$ stores with thapsigargin (Fig. 4) suggested that $Ba^{2+}$ enters that cells *via* a novel pathway. The remaining experiments in the paper were designed to characterize this influx pathway and identify the responsible channels.

The observation that carbachol does not increase the rate of $Mn^{2+}$ influx in thapsigargin- treated cells (Fig. 5), under the same conditions where $Ba^{2+}$ influx is robustly stimulated (Fig. 4C), suggests that the $Ba^{2+}$-permeable (*i.e.*, TRPC6) channels are not permeable to $Mn^{2+}$. This conclusion is in apparent disagreement with the results of Hofmann and coworkers, who used measurements of quenching of fura-2 fluorescence to show that DAG and OAG stimulate $Mn^{2+}$ influx through human TRPC6 channels exogenously expressed in CHO-K1 cells (*23*). Tesfai and coworkers used the same method to show that that OAG stimulates $Mn^{2+}$ influx in PC12 cells (*37*). By contrast, we do not observe the stimulation of $Mn^{2+}$ influx by OAG in PC12D cells under our experimental conditions (Saffen, unpublished observations). This observation suggests that the properties of TRPC6 subtype-containing channels may differ between cell types, even between PC12D and the parental PC12 cells. PC12 sublines have previously been reported to be highly heterogeneous with respect to calcium influx pathways (*38*).

Examination of the dose-response relationship for carbachol-stimulated $Ba^{2+}$ influx shows that there is a good correlation with release of $Ca^{2+}$ from intracellular stores (Fig. 6A), even though $Ca^{2+}$ release itself does not stimulate $Ba^{2+}$ influx (Fig. 4). The estimated $EC_{50}$ for carbachol-stimulation of $Ba^{2+}$ (5 μM) is identical to the $EC_{50}$ for carbachol-stimulation of $IP_3$ release (*24*), suggesting that $Ba^{2+}$ influx depends upon the activation of M1 mAChRs. The observation that both release of $Ca^{2+}$ from internal stores (Fig. 6B) and $Ba^{2+}$ influx (Fig. 6, B and C) are blocked by the PLC inhibitor U73122 is consistent with the involvement of $G_{q/11}$-coupled M1 mAChRs in the activation of the $Ba^{2+}$-permeable channels. Also consistent with the involvement of M1 mAChRs, pretreatment of the cells with pertussis toxin (18 h, 100 ng/ml) had

no effect on $Ba^{2+}$ influx (Guo and Saffen, unpublished observations).

An examination of the dependence of the rate and extent of $Ba^{2+}$ influx as a function of extracellular $Ba^{2+}$ concentration showed that $Ba^{2+}$ accumulation increases with increasing concentrations of extracellular $Ba^{2+}$ (Fig. 7). These results can be explained if the $Ba^{2+}$-permeable channels are, collectively, only transiently activated following stimulation of mAChRs. If the channels remained active for a longer period, it would be expected that different extracellular concentrations of $Ba^{2+}$ would yield the same level of intracellular $Ba^{2+}$, albeit with differing rates of accumulation. The fact that these channels apparently remain open for only 1 to 2 min following exposure carbachol explains why they do not significantly contribute to the extended plateau phase of intracellular $Ca^{2+}$ increases.

The experiment depicted in Fig. 8 shows that $Ba^{2+}$ influx is inhibited by extracellular $Ca^{2+}$. This suggests that the $Ba^{2+}$-permeable channel becomes a $Ca^{2+}$-specific channel in the presence of $Ca^{2+}$. Similar properties have been previously described for other $Ca^{2+}$ channels, including L-type voltage-gated $Ca^{2+}$ channels, which become non-selective cation channels in the absence of extracellular $Ca^{2+}$ (*39*, *40*).

To find a method for pharmacologically distinguishing the $Ba^{2+}$-permeable channels from the SOCCs, we screened a variety of known $Ca^{2+}$ channel blockers and agents known to affect $Ca^{2+}$ channels. These studies showed that the $Ba^{2+}$ permeable channel is blocked at relatively low concentrations of the $Ca^{2+}$ channel inhibitor SK-39365 (Fig. 9). Interestingly, this inhibitor also blocks the background influx of $Ba^{2+}$ in cells not treated with carbachol (Fig. 9, last set of traces). This background $Ba^{2+}$ influx is also observed in cells pretreated with atropine (Figs. 1 and 2), suggesting that $Ba^{2+}$-permeable channels can be activated by pathways not involving mAChR or are constitutively active at low levels. SK-39365 cannot be used to selectively block $Ba^{2+}$ channels in PC12D cells, however, since it also inhibits $Ca^{2+}$ influx through SOCCs at similar concentrations (Guo and Saffen, unpublished observations).

Among the agents we examined, phorbol ester most clearly distinguished the $Ba^{2+}$-permeable channels from the SOCCs, completely blocking the former at low concentrations (Fig. 10), and having no effect on SOCCs (measured as thapsigargin-stimulated $Mn^{2+}$ influx; Guo and Saffen, data not shown). While prolonged incubation of PC12D cells with phorbol ester gradually uncouples muscarinic receptors from PLC-β (Ebihara and Saffen, unpublished observations), this was not observed at the low concentration of phorbol ester and short incubation times used in this study, since there was no apparent loss in carbachol-stimulated release of $Ca^{2+}$ from intracellular stores (Fig. 10). Pretreatment of PC12D cells for short periods of time with phorbol ester did not decrease carbachol-stimulated $Ca^{2+}$ influx (Guo and Saffen, unpublished observations), consistent with the previous conclusion that the $Ba^{2+}$-permeable channels make only a small contribution to carbachol-stimulated $Ca^{2+}$ influx under the experimental conditions used. The fact that inhibition of carbachol-stimulated $Ba^{2+}$ influx by phorbol ester is blocked by low concentrations of GF109203X (Fig. 10, bottom traces) implies that this inhibition is mediated by PKC.

It should be noted that pretreatment of PC12D cells with GF109203X does not increase mAChR-stimulated $Ba^{2+}$ accumulation. This result suggests that the $Ba^{2+}$-permeable channels are also inhibited by PKC-independent mechanisms. One possibility, which remains to be investigated, is that the channels are blocked by increases in intracellular $Ca^{2+}$ (or $Ba^{2+}$). Instead of playing a role in the regulation of $Ba^{2+}$-channels in response to isolated mAChR activations, PKC could function to prevent closely spaced activations of the channel. In this way, phosphorylation by PKC may confer on the channels a "memory" of previous activations.

The results of the antisense and dominant-interfering experiments shown in Figs. 11 and 12 provide evidence that expression of TRPC6 is required for M1 mAChR- and OAG-stimulated $Ba^{2+}$ influx in PC12D cells. As noted above, PC12D cells also express mRNAs for TRPC1, TRPC3 and TRPC7. The possible contributions of these channels to mAChR- and OAG-stimulated $Ba^{2+}$ influx remains to be investigated. TRPC3 and TRPC7 are of particular interest, since they have previously been reported to form heterotetrameric receptors with TRPC6 (*41*, *42*). Determining the molecular composition of the endogenous $Ba^{2+}$-permeable channels in PC12D cells is an important goal for future studies.

The data reported in this and the accompanying paper (Ebihara, Guo, Zhang, Kim and Saffen, 2006) confirm and extend several of the observations of an earlier study, which provided evidence for two independently regulated pathways for $Ca^{2+}$ influx in PC12 cells (*38*). Our results are also consistent with a recent study by Tesfai and coworkers, which showed that OAG stimulates $Ca^{2+}$ influx in PC12 cells and that this influx correlates with the expression of TRPC6 protein (*37*). Unlike our study, however, these authors detected mRNAs for TRPC1–6 (TRPC7 mRNA was not assayed) and found that the OAG stimulated the influx of $Mn^{2+}$. It is unclear whether the OAG-activated channels described in that paper are distinct from the channels described in the present study. PC12 cell sublines have previously been shown to be heterogeneous with respect to mAChR-stimulated $Ca^{2+}$ (*38*), and it is likely that differences in TRPC gene expression and apparent channel permeabilities reflect inter-cell line differences.

In summary, the experiments in this study reveal the presence of a mAChR-regulated $Ba^{2+}$ influx pathway in PC12D cells that is distinct from the store-operated $Ca^{2+}$ influx pathway described in the accompanying paper. These two pathways are mediated by distinct channels that differ in their mechanisms of activation, ion permeabilities, duration of activation and regulation by PKC. While the molecular identity of the SOCCs in PC12D cells is unknown, our data suggests that the $Ba^{2+}$-permeable channels depend upon the expression of TRPC6. An interesting aspect of our model is that these channels may be under dual, and opposing, regulation by DAG: DAG may directly activate the channels on a time scale measured in seconds, but inactivate the channels (via activation of PKC) on a time scale measured in minutes (Fig 13, "fast" and "slow" pathways). A similar bimodal regulation by DAG has been proposed for

TRPC3 channels exogenously expressed in HEK293 cells, which are also transiently activated following stimulation of mAChRs (*43*). A recent study by Trebak and coworkers (*44*) demonstrated that TRPC3 is phosphorylated by PKC on serine$^{712}$, and that this phosphorylation inhibits the activation of the channels. We have recently established that TRPC6 is phosphorylated on the homologous serine residue in TRPC6 (*45*).

Under the experimental conditions used in this study, the SOCCs in PC12D cells make a large and sustained contribution to carbachol-stimulated influx, while the contribution of the TRPC6 channels is small and transient. Saturation of cells with carbachol, however, is probably not representative of physiological cholinergic innervations, which are likely to be spatially restricted to specific small regions of dendrites or cell soma. One can speculate that there are situations where mAChRs may activate $Ca^{2+}$ influx via TRPC6 channels independently of the emptying of the intracellular $Ca^{2+}$ stores. The magnitude of the response would be expected to increase with increasing local concentrations of the TRPC6 channels. Transiently activated TRPC6 channels may have physiological functions that are distinct from the SOCCs, which undergo a sustained activation following activation of mAChRs. A recent study by Delmas and colleagues (*46*) showed that M1 mAChRs in sympathetic neurons activate exogenously expressed TRPC6 channels, but do not stimulate $IP_3$ receptor–mediated release of $Ca^{2+}$ from internal stores. Thus, depending upon the cell type, activation of non-SOCCs may represent a major pathway for M1 mAChR-stimulated $Ca^{2+}$ influx. TRPC6 channels have been shown to be expressed in the developing and adult brain (*47*), and TRPC6 mRNA is expressed at high levels in the granule cells of the dentate gyrus (*48*), which also express M1 mAChRs (*49*). Additional studies will be required to elucidate the possible contributions of TRPC6 and store-operated $Ca^{2+}$ channels to known functions of M1 mAChRs in the brain, including memory, cognition and attention.

This work was supported by Grants-in-Aid (#07279107) for Scientific Research in Priority Areas on "Functional Development of Neural Circuits," the Ministry of Education, Science, Sports and Culture of Japan, the Japan Science and Technology Corporation (CREST), funds from the Department of Pharmacology, Ohio State University and a grant from the Psychiatric Research Foundation, Columbus, Ohio. We thank Tatsuya Haga (Gakushuin University, Tokyo), and Tomoyuki Takahashi (Tokyo University) for critical comments and valuable discussions.

## REFERENCES

1. Schilling, W.P., Rajan, L., and Strobl-Jager, E. (1989) Characterization of the bradykinin-stimulated calcium influx pathway of cultured vascular endothelial cells. Saturability, selectivity, and kinetics. *J. Biol. Chem.* **264**, 12838–12848
2. Kwan, C.Y. and Putney, J.W., Jr. (1990) Uptake and intracellular sequestration of divalent cations in resting and methacholine-stimulated mouse lacrimal acinar cells. Dissociation by $Sr^{2+}$ and $Ba^{2+}$ of agonist-stimulated divalent cation entry from the refilling of the agonist-sensitive intracellular pool. *J. Biol. Chem.* **265**, 678–684
3. Yamaguchi, D.T., Green, J., Kleeman, C.R., and Muallem, S. (1989) Properties of the depolarization-activated calcium and barium entry in osteoblast-like cells. *J. Biol. Chem.* **264**, 197–204
4. Montell, C. (2003) The venerable inveterate invertebrate TRP channels. *Cell Calcium* **33**, 409–417
5. Montell, C., Birnbaumer, L., and Flockerzi, V. (2002) The TRP channels, a remarkably functional family. *Cell* **108**, 595–598
6. Nilius, B. (2003) From TRPs to SOCs, CCEs, and CRACs: consensus and controversies. *Cell Calcium* 33, 293–298
7. Clapham, D.E. (2003) TRP channels as cellular sensors. *Nature* **426**, 517–524
8. Montell, C., Birnbaumer, L., Flockerzi, V., Bindels, R.J., Bruford, E.A., Caterina, M.J., Clapham, D.E., Harteneck, C., Heller, S., Julius, D., Kojima, I., Mori, Y., Penner, R., Prawitt, D., Scharenberg, A.M., Schultz, G., Shimizu, N., and Zhu, M.X. (2002) A unified nomenclature for the superfamily of TRP cation channels. *Mol. Cell* **9**, 229–231
9. Zitt,C.,Zobel,A.,Obukhov,A.G.,Harteneck,C.,Kalkbrenner,F., Luckhoff, A., and Schultz, G. (1996) Cloning and functional expression of a human Ca2+-permeable cation channel activated by calcium store depletion. *Neuron* **16**, 1189–1196
10. Mori, Y., Wakamori, M., Miyakawa, T., Hermosura, M., Hara, Y., Nishida, M., Hirose, K., Mizushima, A., Kurosaki, M., Mori, E., Gotoh, K., Okada, T., Fleig, A., Penner, R., Iino, M., and Kurosaki, T. (2002) Transient receptor potential 1 regulates capacitative $Ca^{2+}$ entry and $Ca^{2+}$ release from endoplasmic reticulum in B lymphocytes. *J. Exp. Med.* **195**, 673–681
11. Vazquez, G., Lievremont, J.P., St, J.B.G., and Putney, J.W., Jr. (2001) Human Trp3 forms both inositol trisphosphate receptor-dependent and receptor-independent store-operated cation channels in DT40 avian B lymphocytes. *Proc. Natl. Acad. Sci. USA* **98**, 11777–11782
12. Trebak, M., Bird, G.S., McKay, R.R., and Putney, J.W., Jr. (2002) Comparison of human TRPC3 channels in receptor-activated and store-operated modes. Differential sensitivity to channel blockers suggests fundamental differences in channel composition. *J. Biol. Chem.* **277**, 21617–21623
13. Vazquez, G., Wedel, B.J., Trebak, M., St John Bird, G., and Putney, J.W., Jr. (2003) Expression level of the canonical transient receptor potential 3 (TRPC3) channel determines its mechanism of activation. *J. Biol. Chem.* **278**, 21649–21654
14. Philipp, S., Trost, C., Warnat, J., Rautmann, J., Himmerkus, N., Schroth, G., Kretz, O., Nastainczyk, W., Cavalie, A., Hoth, M., and Flockerzi, V. (2000) TRP4 (CCE1) protein is part of native calcium release-activated $Ca^{2+}$-like channels in adrenal cells. *J. Biol. Chem.* **275**, 23965–23972
15. Zeng, F., Xu, S.Z., Jackson, P.K., McHugh, D., Kumar, B., Fountain, S.J., and Beech, D.J. (2004) Human TRPC5 channel activated by a multiplicity of signals in a single cell. *J. Physiol.*
16. Riccio, A., Mattei, C., Kelsell, R.E., Medhurst, A.D., Calver, A.R., Randall, A.D., Davis, J.B., Benham, C.D., and Pangalos, M.N. (2002) Cloning and functional expression of human short TRP7, a candidate protein for store-operated $Ca^{2+}$ influx. *J. Biol. Chem.* **277**, 12302–12309
17. Venkatachalam, K., Ma, H.T., Ford, D.L., and Gill, D.L. (2001) Expression of functional receptor-coupled TRPC3 channels in DT40 triple receptor InsP3 knockout cells. *J. Biol. Chem.* **276**, 33980–33985
18. Fasolato, C., Zottini, M., Clementi, E., Zacchetti, D., Meldolesi, J., and Pozzan, T. (1991) Intracellular $Ca^{2+}$ pools in PC12 cells. Three intracellular pools are distinguished by their turnover and mechanisms of $Ca^{2+}$ accumulation, storage, and release. *J. Biol. Chem.* **266**, 20159–20167
19. Plant, T.D. and Schaefer, M. (2003) TRPC4 and TRPC5: receptor-operated $Ca^{2+}$-permeable nonselective cation channels. *Cell Calcium* **33**, 441–450
20. Boulay, G., Zhu, X., Peyton, M., Jiang, M., Hurst, R., Stefani, E., and Birnbaumer, L. (1997) Cloning and expression

of a novel mammalian homolog of *Drosophila* transient receptor potential (Trp) involved in calcium entry secondary to activation of receptors coupled by the Gq class of G protein. *J. Biol. Chem.* **272**, 29672–29680
21. Zhang, L. and Saffen, D. (2001) Muscarinic acetylcholine receptor regulation of TRP6 $Ca^{2+}$ channel isoforms. Molecular structures and functional characterization. *J. Biol. Chem.* **276**, 13331–13339
22. Okada, T., Inoue, R., Yamazaki, K., Maeda, A., Kurosaki, T., Yamakuni, T., Tanaka, I., Shimizu, S., Ikenaka, K., Imoto, K., and Mori, Y. (1999) Molecular and functional characterization of a novel mouse transient receptor potential protein homologue TRP7. $Ca^{2+}$-permeable cation channel that is constitutively activated and enhanced by stimulation of G protein-coupled receptor. *J. Biol. Chem.* **274**, 27359–27370
23. Hofmann, T., Obukhov, A.G., Schaefer, M., Harteneck, C., Gudermann, T., and Schultz, G. (1999) Direct activation of human TRPC6 and TRPC3 channels by diacylglycerol. *Nature* **397**, 259–263
24. Ebihara, T. and Saffen, D. (1997) Muscarinic acetylcholine receptor-mediated induction of zif268 mRNA in PC12D cells requires protein kinase C and the influx of extracellular calcium. *J. Neurochem.* **68**, 1001–1010
25. Avidor, B., Avidor, T., Schwartz, L., De Jongh, K.S., and Atlas, D. (1994) Cardiac L-type $Ca^{2+}$ channel triggers transmitter release in PC12 cells. *FEBS Lett.* **342**, 209–213
26. Usowicz, M.M., Porzig, H., Becker, C., and Reuter, H. (1990) Differential expression by nerve growth factor of two types of $Ca^{2+}$ channels in rat phaeochromocytoma cell lines. *J. Physiol.* **426**, 95–116
27. Liu, H., Felix, R., Gurnett, C.A., De Waard, M., Witcher, D.R., and Campbell, K.P. (1996) Expression and subunit interaction of voltage-dependent $Ca^{2+}$ channels in PC12 cells. *J. Neurosci.* **16**, 7557–7565
28. Crespo, L.M., Grantham, C.J., and Cannell, M.B. (1990) Kinetics, stoichiometry and role of the Na-Ca exchange mechanism in isolated cardiac myocytes. *Nature* **345**, 618–621
29. Rosker, C., Graziani, A., Lukas, M., Eder, P., Zhu, M.X., Romanin, C., and Groschner, K. (2004) $Ca^{2+}$ signaling by TRPC3 involves $Na^+$ entry and local coupling to the $Na^+/Ca^{2+}$ exchanger. *J. Biol. Chem.* **279**, 13696–13704
30. Reeves, J.P., Chernaya, G., and Condrescu, M. (1996) Sodium-calcium exchange and calcium homeostasis in transfected Chinese hamster ovary cells. *Ann. NY Acad. Sci.* **779**, 73–85
31. Condrescu, M., Chernaya, G., Kalaria, V., and Reeves, J.P. (1997) Barium influx mediated by the cardiac sodium-calcium exchanger in transfected Chinese hamster ovary cells. *J. Gen. Physiol.* **109**, 41–51
32. van Koppen, C.J. and Kaiser, B. (2003) Regulation of muscarinic acetylcholine receptor signaling. *Pharmacol. Ther.* **98**, 197–220
33. Smith, R.J., Sam, L.M., Justen, J.M., Bundy, G.L., Bala, G.A., and Bleasdale, J.E. (1990) Receptor-coupled signal transduction in human polymorphonuclear neutrophils: effects of a novel inhibitor of phospholipase C-dependent processes on cell responsiveness. *J. Pharmacol. Exp. Ther.* **253**, 688–697
34. Thompson, A.K., Mostafapour, S.P., Denlinger, L.C., Bleasdale, J.E., and Fisher, S.K. (1991) The aminosteroid U-73122 inhibits muscarinic receptor sequestration and phosphoinositide hydrolysis in SK-N-SH neuroblastoma cells. A role for Gp in receptor compartmentation. *J. Biol. Chem.* **266**, 23856–23862
35. Grynkiewicz, G., Poenie, M., and Tsien, R.Y. (1985) A new generation of Ca2+ indicators with greatly improved fluorescence properties. *J. Biol. Chem.* **260**, 3440–3450
36. Merritt, J.E., Armstrong, W.P., Benham, C.D., Hallam, T.J., Jacob, R., Jaxa-Chamiec, A., Leigh, B.K., McCarthy, S.A., Moores, K.E., and Rink, T.J. (1990) SK&F 96365, a novel inhibitor of receptor-mediated calcium entry. *Biochem. J.* **271**, 515–522
37. Tesfai, Y., Brereton, H.M., and Barritt, G.J. (2001) A diacylglycerol-activated $Ca^{2+}$ channel in PC12 cells (an adrenal chromaffin cell line) correlates with expression of the TRP-6 (transient receptor potential) protein. *Biochem. J.* **358**, 717–726
38. Clementi, E., Scheer, H., Zacchetti, D., Fasolato, C., Pozzan, T., and Meldolesi, J. (1992) Receptor-activated $Ca^{2+}$ influx. Two independently regulated mechanisms of influx stimulation coexist in neurosecretory PC12 cells. *J. Biol. Chem.* **267**, 2164–2172
39. Almers, W. and McCleskey, E.W. (1984) Non-selective conductance in calcium channels of frog muscle: calcium selectivity in a single-file pore. *J. Physiol.* **353**, 585–608
40. Almers, W., McCleskey, E.W., and Palade, P.T. (1984) A non-selective cation conductance in frog muscle membrane blocked by micromolar external calcium ions. *J. Physiol.* **353**, 565–583
41. Hofmann, T., Schaefer, M., Schultz, G., and Gudermann, T. (2002) Subunit composition of mammalian transient receptor potential channels in living cells. *Proc. Natl. Acad. Sci. USA* **99**, 7461–7466
42. Goel, M., Sinkins, W.G., and Schilling, W.P. (2002) Selective association of TRPC channel subunits in rat brain synaptosomes. *J. Biol. Chem.* **277**, 48303–48310
43. Venkatachalam, K., Zheng, F., and Gill, D.L. (2003) Regulation of TRPC channel function by diacylglycerol and protein kinase C. *J. Biol. Chem.* **278**, 29031–29340
44. Trebak, M., Hempel, N., Wedel, B.J., Smyth, J.T., Bird, G.S., and Putney, J.W., Jr. (2005) Negative regulation of TRPC3 channels by protein kinase C-mediated phosphorylation of serine 712. *Mol. Pharmacol.* **67**, 558–563
45. Kim, J.Y. and Saffen, D. (2005) Activation of M1 muscarinic acetylcholine receptors stimulates the formation of a multiprotein complex centered on TRPC6 channels. *J. Biol. Chem.***280**, 32035–32047
46. Delmas, P., Wanaverbecq, N., Abogadie, F.C., Mistry, M., and Brown, D.A. (2002) Signaling microdomains define the specificity of receptor-mediated InsP(3) pathways in neurons. *Neuron* **34**, 209–220
47. Strubing, C., Krapivinsky, G., Krapivinsky, L., and Clapham, D.E. (2003) Formation of novel TRPC channels by complex subunit interactions in embryonic brain. *J. Biol. Chem.* **278**, 39014–39019
48. Mizuno, N., Kitayama, S., Saishin, Y., Shimada, S., Morita, K., Mitsuhata, C., Kurihara, H., and Dohi, T. (1999) Molecular cloning and characterization of rat trp homologues from brain. *Brain Res. Mol. Brain Res.* **64**, 41–51
49. Volpicelli, L.A. and Levey, A.I. (2004) Muscarinic acetylcholine receptor subtypes in cerebral cortex and hippocampus. *Prog. Brain Res.* **145**, 59–66